CLM-P356

E·MINIMIS·MAXIMA

UKAEA RESEARCH GROUP

Preprint

SATELLITE SPECTRA FOR HELIUM-LIKE IONS IN LASER-PRODUCED PLASMAS

N J PEACOCK
M G HOBBY
M GALANTI

CULHAM LABORATORY
Abingdon Berkshire

1973

CLM-P 356

SATELLITE SPECTRA FOR HELIUM-LIKE IONS IN LASER-PRODUCED PLASMAS

by

N J Peacock, M G Hobby* and M Galanti†

(submitted for publication in J.Phys.B, Atom.Molec.Phys.)

ABSTRACT

Satellites to the resonance lines of helium-like ions are distinctive features of the spectra from high-pressure plasmas such as those produced in the absorption layer of a high-intensity laser beam incident on a solid surface. The satellites are spatially coincident with the free-bound continua into the helium-like ions and are produced mainly by dielectronic recombination. Their wavelengths are identified by comparison with Hartree-Fock-type calculations. The intensities of some of the dielectronic satellites increase anomalously with the atomic charge of the ion.

* Attached from Leicester University

† ESRO Fellow, attached from Imperial College, London

UKAEA Research Group
Culham Laboratory
Abingdon
Berks.

September 1973

Emission lines situated on the long wavelength side of the allowed resonance lines of helium-like ions were first reported by Edlén and Tyrén (1939) who ascribed them to screened transitions of the type $1s^2 n\ell - 1s2pn\ell$ and $1s^2 n\ell - 1s2sn\ell$ in lithium-like ions, transitions with $n=2$ being responsible for the most prominent lines. More recently these lines have been shown to be distinctive features of solar flare spectra, for example the emission from Mg XI reported by Parkinson (1972). Ion species up to Ni XXVII have been recorded in the solar spectrum and until now this has proved to be the most useful source of these lines. Satellites have also been observed in high-temperature laboratory plasmas such as the Plasma Focus where the spectrum of A XVII has been analysed by Peacock et al (1971). Schwob and Fraenkel (1972) have reported the spectrum of Fe XXV and its satellites from a low inductance vacuum spark. In these laboratory sources even using crystal instruments of high resolving power the discrimination between satellite components tends to be limited by source broadening.

It is the purpose of this paper to report that plasmas produced at solid surfaces as a result of intense laser irradiation are also powerful sources for studying the spectra from highly-stripped ions. By varying the target element and the laser intensity isoelectronic sequences of the satellite structure can be constructed readily.

The intensities of the helium-like ion lines and their satellites vary with ionising conditions in the plasma and it has been pointed out by Gabriel and Jordan (1969) that in the steady state the upper levels of the satellites are populated primarily by dielectronic recombination, though direct inner-shell excitation can also contribute in rapidly ionising conditions. Interspersed through the dielectronic satellite lines there often appear on the long wavelength side of the allowed line the intercombination line $1s^2\ {}^1S_0 - 1s2p\ {}^3P_1$ and the forbidden line $1s^2\ {}^1S_0 - 1s2s\ {}^3S_1$. The intensity of the latter is comparable to that of the allowed line in solar flares. A theoretical treatment of the intensities of all of these lines is given by Gabriel and Jordan (1971) and by Gabriel (1972). Using this theoretical basis the parameters of a plasma and its ionising conditions can be evaluated satisfactorily as in the case of the Plasma Focus (Peacock and Hobby, 1973).

A study of the plasma produced at surfaces irradiated by an intense neodymium laser beam (Galanti and Peacock, 1973) has shown that, for a polythene target, the absorption layer of the incident light is of the order of 10 microns wide with a mean electron density of $4 \times 10^{20}\ cm^{-3}$. This layer is spatially defined by high-temperature free-bound continua into H-like and He-like ions and by their satellite line spectra. This is in contrast to the region emitting the allowed lines of the He-like ions, for example, which extends many millimetres from the target surface. Both the electron temperature, T_e, and the product of the density and ion heating time, $n\tau$, increase with the laser flux intensity (Galanti and Peacock, 1973), so that species of considerably higher ionisation can be anticipated with laser flux intensities which exceed those used here. In this work spectra from the He-like ions C V, F VIII, Mg XI and Al XII have been produced by irradiating appropriate plane, solid targets with a 4.5 nanosecond neodymium laser pulse which has a peak intensity variable up to 5×10^{12} watts/cm^2 at the target surface. The satellite spectra have been recorded with spatial resolution using grating and crystal dispersion over the wavelength range from a few Angstroms to fifty Angstroms. The wavelengths of the satellite lines and their relative intensities and identifications are shown in Table 1. Classification of the terms responsible for these lines has been facilitated by Hartree-Fock type calculations, initially by Cowan (1969), and later by Gabriel (1972) and Vainshtein and Safronova (1971). A summary of theoretical classifications and intensities for the satellites is given in Gabriel (1972) and we follow the convenient key-letter identification used in that paper. We illustrate some anomalous intensities in the observed satellite features by referring to the spectra of C V, Figure 1, and Mg XI, Figure 2.

In the spectrum of the carbon plasma the intense satellite group "a - d" is $1s^22p\ ^2P - 1s2p^2\ ^2P^e$, the upper levels of which are populated, not by dielectronic recombination, for reasons of parity, but directly from the Li-like ion. The neighbouring satellites "q,r" and "j,k,l" are readily attributable to the $1s2s2p\ ^2P^o$ and $1s2p^2\ ^2D^e$ terms which are populated by dielectronic recombination of the He-like ion. The theoretical intensities of these dielectronic satellites are equal (Gabriel, 1972) and this is confirmed by observation. In the magnesium spectrum, however, it is apparent that the intercombination lines "x,y" and the satellites "j,k,l" are equal in intensity and a much larger fraction of the allowed line "w" than in carbon. The increase in intensity of both of these features with the effective atomic charge, Z, on the ion is a notable observation along the isoelectronic sequence, Table 1. For the intercombination line intensity, where the transition probability scales as Z^9, this is understandable; however there is no good reason why the dielectronic satellites "j,k,l" should also scale as a steep function of Z. In the Al XII satellite for example, the intensity of the "j,k,l," feature already exceeds that of the intercombination line and is almost 70% of the resonance line intensity. It is interesting to note that these satellites "j,k,l," are, with the present wavelength resolution, coincident with the helium ion forbidden line "z", $1s^2\ ^1S_0 - 1s2s\ ^3S_1$, throughout the whole isoelectronic sequence. This is illustrated in Figure 3. One would expect any contribution from the forbidden line to increase rapidly with the atomic charge since the transition probability scales as Z^{10}.

On the other hand Gabriel and Jordan (1971) have pointed out that the forbidden line intensity will be a very critical function of the electron density, n_e, and will only equal the intercombination line intensity for the Mg $\overline{\underline{XI}}$ ion at a low value $n_e \simeq 2 \times 10^{13}$ cm^{-3}. For the much higher densities of the absorption layer its intensity should be negligible since $A\ (1s^2\ {}^1S_0 - 1s2s\ {}^3S_1) \ll n_e\ C\ (1s2s\ {}^3S \leftrightarrow 1s2s\ {}^3P) < \tau^{-1}$, where C is the collisional term.

Attempts to attribute the intensity of the satellite feature "z - j,k,l" to the forbidden line and to explain its intensity on grounds of super-radiance, on Zeeman splitting in the high magnetic fields recorded in laser plasmas (Stamper et al, 1971), on Stark broadening or on optical opacity (the allowed line is optically thick) have not yet met with success. Certainly we expect the intensity of this feature to be dependent on the plasma conditions rather than on atomic constants, since the $1s2p^2\ {}^2D^e$ satellite has no enhanced intensity in the A $\overline{\underline{XVII}}$ spectrum produced in the Plasma Focus where the density is $\sim 10^{19}$ cm^{-3} (Peacock and Hobby, 1973).

Finally, in order to illustrate the capacity of the laser produced plasma for producing a high population of excited levels we include an analysis of new fluorine spectra between 60 and 140 Å in Table 2.

We wish to acknowledge the assistance of A H Jones in the operation of the laser.

References

Cowan R. D., 1969, Private Communication, Los Alamos.

Edlén B. and Tyrén F., 1939, Nature, 143, 940.

Gabriel A. H. and Jordan C., 1969, Nature, 221, 947-949.

Gabriel A. H. and Jordan C., 1971, "Case Studies in Atomic Collision Physics", Vol. 2, Chapter 4, Editors McDaniel and McDowell, North Holland Publishers.

Gabriel A. H., 1972, Mon. Not. Roy. Ast. Soc., 160,99-119.

Galanti M. and Peacock N. J., 1973, Proc. 6th European Conf. on Controlled Fusion and Plasma Physics, Moscow USSR, Vol. 1, 427-430.

Garcia J. D. and Mack J. E., 1965, J. Opt. Soc. Am., 55, 654-685.

Neupert W., 1971, Solar Phys., 18, 474-488.

Parkinson J. H., 1972, Nature, 236, 68-71.

Peacock N. J., Hobby M. G. and Morgan P. D., 1971, "Plasma Physics and Controlled Fusion", Vol. 1, 537-551, IAEA Vienna.

Peacock N. J., and Hobby M. G., 1973, to be published.

Sawyer G. A., Jahoda F. C., Ribe F. L., and Stratton T. F., 1962, J. Quant. Spec. Rad. Trans., 2, 467-475.

Schwob J. L., and Fraenkel B. S., 1972, Space Science Rev., 13, 589-591.

Stamper J. A., Papadopoulos K., Sudan R. N., Dean S. O., and McLean E. A., 1971, Phys. Rev. Lett., 26, 1012-1015.

Vainshtein L. A., and Safronova U. I., 1971, Sov. Astr., 15, 175-176.

Walker A. B. C., and Rugge H. R., 1971, Ap. J., 164, 181-186.

TABLE 1. Wavelengths and intensities of lines indentified in laser-produced plasmas. The key letters are those designated by Gabriel (1972).

*Gabriel(1972), +Garcia and Mack(1965), ‡Neupert(1971), ø Cowan(1969), † Sawyer et al(1962), ≠ Walker and Rugge(1971).

Classification	Key	Carbon			Fluorine			Magnesium			Aluminium		
		λobs Å	λcalc Å	I	λobs Å	λcalc Å	I	λobs Å	λcalc Å	I	λobs Å	λcalc Å	I
H-like													
$1s\ ^2S_{1/2}$ - $2p\ ^2P_{1/2,3/2}$					14.984	14.984+	111	8.43	8.421+	2			
3p					12.644	12.644+	45						
4p					11.985	11.988+	25						
5p					11.704	11.707+	10						
6p					11.555	11.560+	4						
He-like													
$1s^2\ ^1S_0$ - $1s2s\ ^3S_1$	(z)		41.47*		blend [17.151]	17.152*	23	blend [9.316]	9.314*	32	blend [7.873]	7.871*	66
$1s2p\ ^1P_1$	(w)	40.27	40.27*	100	16.804	16.805*	100	9.168	9.168*	100	7.757	7.756*	100
$1s2p\ ^3P_2$	(x)	40.73	40.73*	6	16.952	16.949*	15	9.230	9.228*	31	7.806	7.804*	36
$1s2p\ ^3P_1$	(y)					16.952*			9.231*			7.807*	
$1s3p\ ^1P_1$					14.460	14.46†	52	7.850	7.85‡	8	6.637	6.635≠	10
1s4p					13.783	17.78†	35	7.473	7.48‡	4			
1s5p					13.494	13.49†	20	7.300		3			
1s6p					13.338		8						
1s7p					13.27		4						
$1s2s\ ^1S_0$ - $2s2p\ ^1P_1$		34.29	34.277ø	5									
$^3S_1$ $^3P_2$		34.52	34.519ø	8	15.217	15.215ø	6						
$1s2p\ ^1P_1$ - $2p^2\ ^1D_2$		34.69	34.650ø	8	15.280	15.273ø	8						
^3P ^3P		34.58	34.590ø	9									
$1s3s\ ^3S$ - $2p3s\ ^3P$		33.93		3									
^1S ^1P		34.04		3									
Li-like													
$1s^22s\ ^2S_{1/2}$ - $1s2s2p(^1P)\ ^2P_{3/2}$	(q)	41.34	41.33*	8	17.084	17.093*	13	9.282	9.284*	16	7.847	7.846*	14
$^2P_{1/2}$	(r)					17.095*			9.286*			7.848*	
$1s2s3p(^1P)\ ^2P^0$		36.73	36.798ø	3									
$1s2s4p(^1P)\ ^2P^0$		35.56	35.533ø	1									
$1s2s2p(^3P)\ ^2P_{3/2}$	(s)	40.86	40.79*	5		16.964*		9.243	9.235*	4	7.815	7.809*	11
$^2P_{1/2}$	(t)					16.965*			9.236*			7.810*	
$1s2s3p(^3P)\ ^2P^0$		36.28	36.294ø	2				8.07	8.055ø	2	6.83	6.810ø	5
$1s^22p\ ^2P_{1/2}$ - $1s2p^2\ ^2S_{1/2}$	(n)		40.60*			16.921*		9.219	9.218*	4	7.787	7.796*	8
$^2P_{3/2}$ $^2S_{1/2}$	(m)					16.924*			9.221*			7.799*	
$^2P_{1/2}$ $^2P_{3/2}$	(b)					17.116*			9.292*			7.853*	
$^2P_{3/2}$ $^2P_{3/2}$	(a)	41.37	41.38*	8	17.107	17.118*	10	9.294	9.296*	13	7.854	7.856*	11
$^2P_{1/2}$ $^2P_{1/2}$	(d)					17.119*			9.296*			7.856*	
$^2P_{3/2}$ $^2P_{1/2}$	(c)					17.121*			9.299*			7.860*	
$^2P_{1/2}$ $^2D_{3/2}$	(k)					17.165*			9.318*			7.874*	
$^2P_{3/2}$ $^2D_{5/2}$	(j)	41.55	41.55*	7	blend [17.15]	17.168*	23	blend [9.316]	9.321*	32	blend [7.873]	7.877*	66
$^2P_{3/2}$ $^2D_{3/2}$	(1)					17.168*			9.322*			7.878*	
$1s2p3p\ ^2S$		36.90	36.929ø	3									
^2P		37.19	37.193ø	3									
^2D		37.02	37.011ø	3									
$1s2p4p\ ^2D$		35.78	35.769ø	1									
$1s^2n\ell$ - $1s2pn\ell$ $n \geq 3$		40.40		5	16.84		5	9.181		5	7.765		10
		40.47		5				9.187		4	7.772		10
								9.195		3	7.827		5
								9.266		2			

TABLE 2

Spectra of F VII and F VIII as measured from laser produced plasmas

λ (Å)	Intensity	Calculated λ (Å)	Identification
F VIII			
*98.799	10		1s2p ^2P - 1s 3d ^3D
*98.707			
73.83	8	73.83 ± 0.01	4d
66.13	6	66.13 ± 0.04	5d
62.55	4	62.52 ± 0.03	6d
60.62	3	60.60 ± 0.05	7d
59.38	2	59.41 ± 0.05	8d
93.23	8	93.27 ± 0.02	1s2s ^3S - 1s 3p ^3P
70.41	6	70.42 ± 0.04	4p
63.26	4	63.24 ± 0.01	5p
60.28	3	60.28 ± 0.05	6p
F V11			
*134.882	5		$1s^22p$ ^2P - $1s^23s$ ^2S
*134.703			
97.36	5	97.36 ± 0.05	4s
97.26	4	97.23 ± 0.03	4s
86.47	3	86.44 ± 0.03	5s
*127.796	10		$1s^22p$ ^2P - $1s^23d$ ^2D
*127.653			
* 95.775	10		4d
* 95.697			
85.80	9	85.82 ± 0.01	5d
81.18	7	81.24 ± 0.02	6d
78.66	5	78.72 ± 0.04	7d
77.08	4	77.13 ± 0.05	8d
76.05	2	76.10 ± 0.05	9d
*112.976	10		$1s^22s$ ^2S - $1s^2$ 3p ^2D
*112.935			
* 86.728	9		4p
78.36	7	78.35 ± 0.02	5p
74.47	5	74.49 ± 0.01	6p
72.30		72.32 ± 0.03	7p
71.00	2	70.94 ± 0.05	8p

* Previous observations

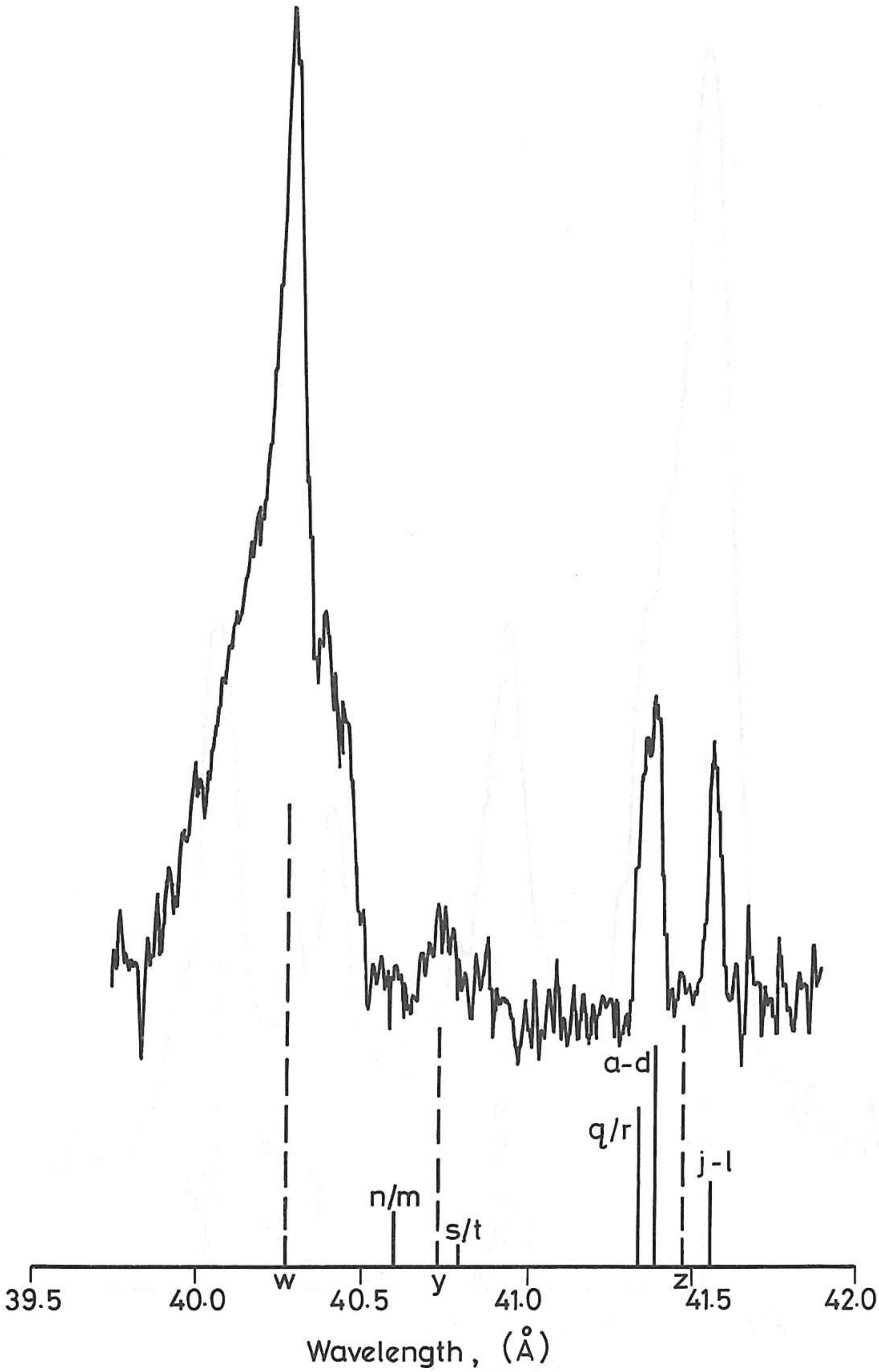

Fig. 1 Grazing incidence grating spectrum from a laser-produced plasma showing the C V He-like ion emission and the associated long wavelength satellites. The vertical lines represent the theoretical spectrum computed by Gabriel (1972) and the key letters are those designated there. Broken lines are due to the He-like ion and solid lines to the Li-like satellites, their heights being proportional to the computed transition probabilities. Neodymium-doped glass laser flux density ~2×10^{12} watts/cm^2 on a polythene target.

CLM-P356

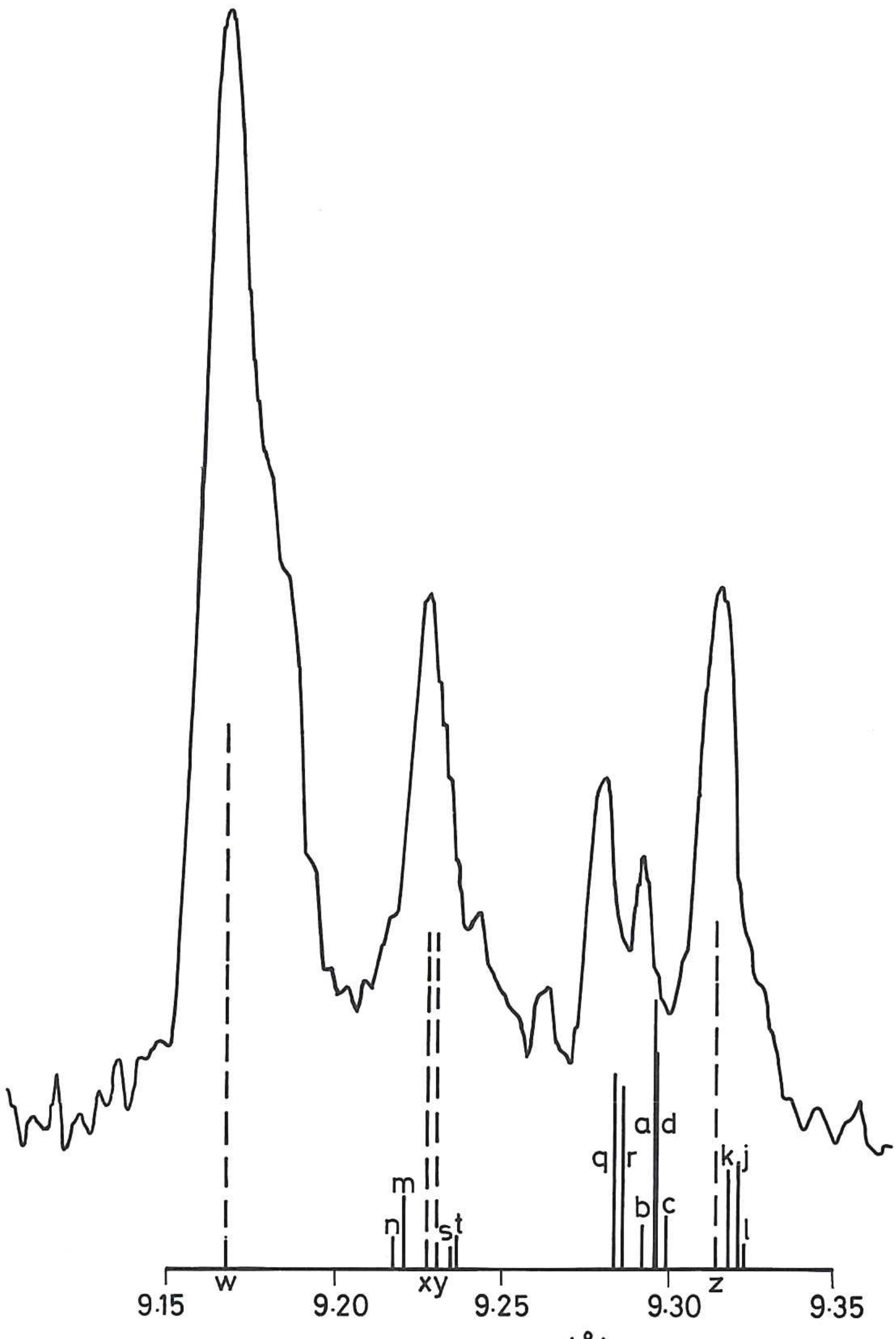

Fig. 2 Curved mica crystal spectrum from a laser-produced plasma comparing the Mg $\overline{XI}$ He-like ion emission and associated long wavelength satellites with the computed spectrum. Laser flux density ~2×10^{12} watts/cm^2 on a pure magnesium target.

CLM-P356

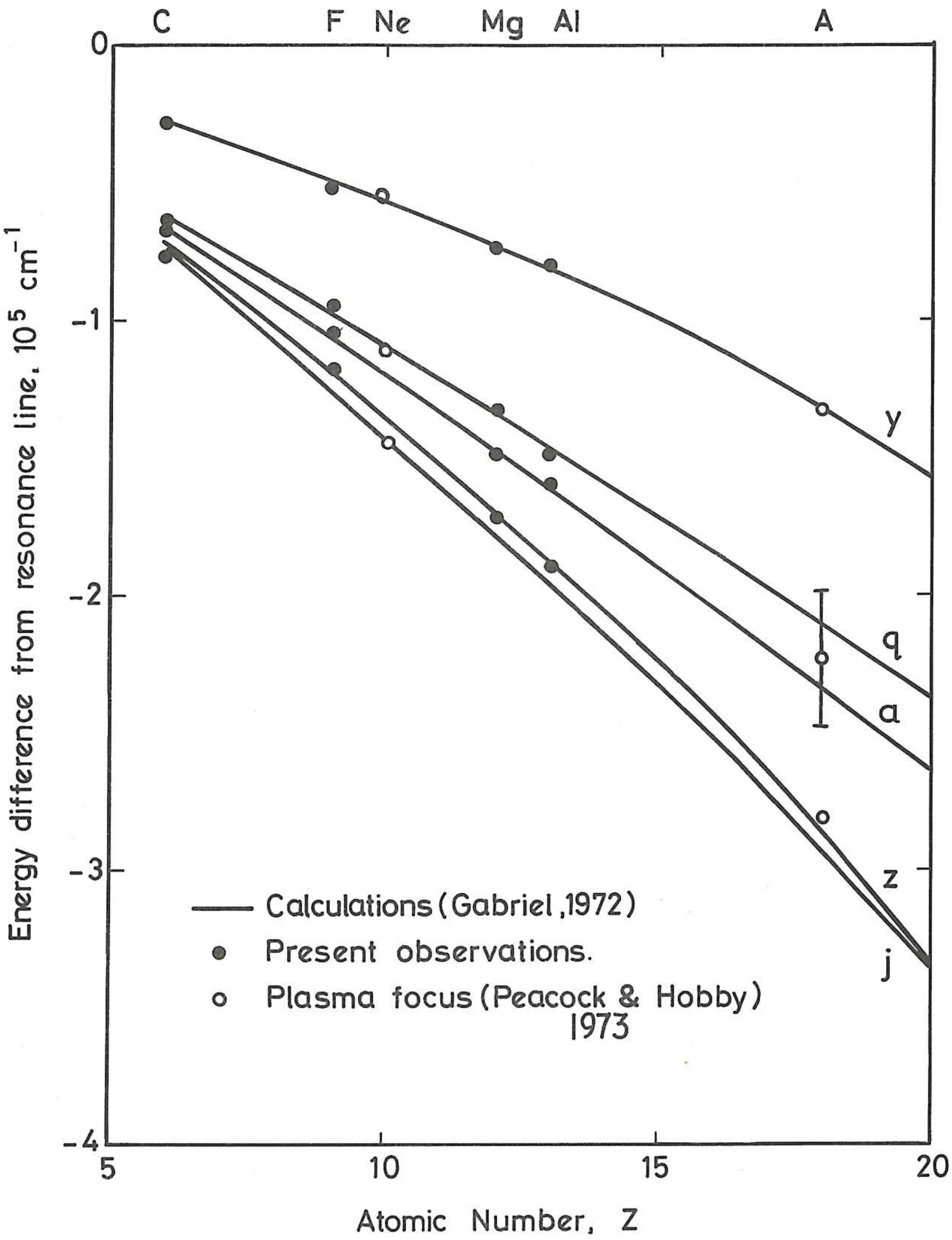

Fig. 3 Isoelectronic sequence of the energy difference between Li-like satellites and the He-like resonance line. The key letters are those designated by Gabriel (1972).
In the Plasma Focus the lines are broadened by instrumental and Doppler effects. The extent of the broadening is indicated in the argon case.